phys. stat. sol. (c) **2**, No. 9, 3500–3504 (2005) / **DOI** 10.1002/pssc.200461236

Modeling Raman scattering in porous silicon

Miguel Cruz[1] and **Chumin Wang**[*2]

[1] Sección de Estudios de Posgrado, ESIME-Culhuacan, IPN, Av. Santa Ana 1000, 04430, México, D.F., México
[2] Instituto de Investigaciones en Materiales, UNAM, A.P. 70-360, 04510, México, D.F., México

Received 20 August 2004, revised 25 November 2004, accepted 27 January 2005
Published online 9 June 2005

PACS 63.22.+m, 78.30.Am

In this work, we model the Raman scattering by phonons using the Born potential and the Green's function formalism, which takes into account the long-range correlation of atomic vibrations. The porous silicon is viewed as a sponge, in which periodical column pores are dug in direction [001] from crystalline silicon, *i.e.*, a supercell model is used to calculate the Raman response. The results show that the main Raman peak shifts to lower energies when the porosity increases, and for square pores it asymptotically approaches to a limit value of 475 cm^{-1}. Finally, the supercell results are compared with the quantum wire model, in which the main Raman peaks move to higher energies as the width of the wires grows.

1 Introduction

Raman scattering study is a very powerful tool for investigating the composition, bonding, and structural properties of solids [1]. However, the fundamental electronic processes involved in the Raman scattering are complicated to describe theoretically. In general, the Raman response depends on the local polarization of the bonds due to the atomic motions. Considering the model of the polarisability tensor developed by Alben *et al.* [2], in which the local bond polarisabilities, $\alpha(l)$, are supposed to be linear with the atomic displacements $u_\mu(l)$, *i.e.,* $c_\mu(l) = \partial\alpha(l)/\partial u_\mu(l)$ alternates only in sign from site to site in a single crystal with diamond structure, the Raman response $R(\omega)$ is proportional to [3, 4]

$$R(\omega) \sim -\omega\, c^2\, \mathrm{Im} \sum_{\mu,\mu'} \sum_{l,l'} (-1)^{l-l'} G_{\mu\mu'}(l,l',\omega)\,, \tag{1}$$

where $\mu, \mu' = x, y, z$ and $G_{\mu\mu'}(l,l',\omega) = \langle\langle u_\mu(l); u_{\mu'}(l') \rangle\rangle$ is the displacement-displacement Green's function and satisfies the Dyson's equation:

$$M\omega^2 G_{\mu\mu'}(l,l',\omega) = \delta_{\mu,\mu'}\delta_{l,l'} + \sum_{\mu''} \sum_{l''} \Phi_{\mu\mu''}(l,l'')\; G_{\mu''\mu'}(l'',l',\omega)\,. \tag{2}$$

Within the Born model, the interactions between nearest-neighbor atoms can be written as [5]

$$V_{ll'} = \frac{1}{2}(\alpha - \beta)\{[\boldsymbol{u}(l) - \boldsymbol{u}(l')] \cdot \hat{\boldsymbol{n}}_{ll'}\}^2 + \frac{1}{2}\beta |\boldsymbol{u}(l) - \boldsymbol{u}(l')|^2\,, \tag{3}$$

* Corresponding author: e-mail: chumin@servidor.unam.mx, Phone: +52-55-56224634, Fax: +52-55-56161251

where α is the restoring force constant along the unit vector $\hat{\boldsymbol{n}}_{ll'}$ that the joints the two neighboring sites l,l', and β is a non-central force constant. For the case of crystalline silicon (*c*-Si), the force constants are $\alpha = 120.3$ Nm^{-1} and $\beta = 23.5$ Nm^{-1} [5]. Therefore, the dynamical matrix ($\boldsymbol{\Phi}$) is given by

$$\phi_{\mu\mu'}(l,l') = \frac{\partial^2 V_{ll'}}{\partial u_{\mu}(l)\partial u_{\mu'}(l')} \quad . \tag{4}$$

In particular, if z-axis of $\boldsymbol{u}(l)-\boldsymbol{u}(l')$ is choose along the union of neighbor sites *l* and *l'*, the Born interaction matrix ($\boldsymbol{\Phi}$) has a very simple form

$$\boldsymbol{\Phi} = -\begin{pmatrix} \beta & 0 & 0 \\ 0 & \beta & 0 \\ 0 & 0 & \alpha \end{pmatrix}. \tag{5}$$

However, since ϕ should be written in the reference of *c*-Si, it is necessary to make appropriate rotations of ϕ. For tetrahedral solids there are four kinds of interaction matrix, and they are

$$\boldsymbol{\Phi}_{x_1} = \begin{pmatrix} -d_1 & \frac{d_2}{\sqrt{2}} & \frac{d_2}{\sqrt{2}} \\ \frac{d_2}{\sqrt{2}} & -\frac{1}{2}(\beta+d_3) & \frac{1}{2}(\beta-d_3) \\ \frac{d_2}{\sqrt{2}} & \frac{1}{2}(\beta-d_3) & -\frac{1}{2}(\beta+d_3) \end{pmatrix}, \quad \boldsymbol{\Phi}_{x_2} = \begin{pmatrix} -d_1 & -\frac{d_2}{\sqrt{2}} & -\frac{d_2}{\sqrt{2}} \\ -\frac{d_2}{\sqrt{2}} & -\frac{1}{2}(\beta+d_3) & \frac{1}{2}(\beta-d_3) \\ -\frac{d_2}{\sqrt{2}} & \frac{1}{2}(\beta-d_3) & -\frac{1}{2}(\beta+d_3) \end{pmatrix},$$

$$\boldsymbol{\Phi}_{y_1} = \begin{pmatrix} -\beta & 0 & 0 \\ 0 & -(d_1-2d_2+d_3)/2 & (d_1-d_3)/2 \\ 0 & (d_1-d_3)/2 & -(d_1-2d_2+d_3)/2 \end{pmatrix},$$

and

$$\boldsymbol{\Phi}_{y_2} = \begin{pmatrix} -\beta & 0 & 0 \\ 0 & -(d_1+2d_2+d_3)/2 & (d_1-d_3)/2 \\ 0 & (d_1-d_3)/2 & -(d_1-2d_2+d_3)/2 \end{pmatrix}, \tag{6}$$

where

$$d_1 = \beta\cos^2\frac{1}{2}\theta + \alpha \ \ \mathrm{sen}^2\frac{1}{2}\theta\,,$$

$$d_2 = (\alpha-\beta)\cos\frac{1}{2}\theta \ \ \mathrm{sen}\frac{1}{2}\theta\,,$$

$$d_3 = \alpha\cos^2\frac{1}{2}\theta + \beta \ \ \mathrm{sen}^2\frac{1}{2}\theta\,,$$

and the angle between tetrahedral bonds is $\theta = \cos^{-1}(-1/3)$. For tetrahedral structures it is easy to prove that

$$\boldsymbol{\Phi}_{x_1} + \boldsymbol{\Phi}_{x_2} + \boldsymbol{\Phi}_{y_1} + \boldsymbol{\Phi}_{y_2} = -\frac{4}{3}(\alpha+2\beta)\boldsymbol{I}\,, \tag{7}$$

where **I** is the matrix identity.

In the last years, the nanocrystalline structures of porous silicon (PSi) layers have been extensively studied using the Raman scattering technique [6]. In this paper we apply the supercell approach to calculate phonon band structures and the Raman response, where the pores are produced by removing columns of Si atoms in [001] direction, dug into an otherwise *c*-Si. This approach has the advantage of being simple and emphasizing the interconnection feature of the system, in contrast with the quantum wire model. In the next section we present the Raman scattering calculations by means of the Born model with central and non-central forces, and the supercell-approach results will be compared with those obtained from the quantum wire model.

2 Results and discussion

The phonon dispersion relations are shown in Fig. 1(a) for *c*-Si and in figure 1(b) for PSi, modeled by an 8-atom supercell containing a two-atom column pore. Observe the flattening bands and the appearance of states due to dangling bonds in Fig. 1(b), similar to the electron case [7]. Furthermore, a significant reduction of the optical mode frequency about 31.8 cm^{-1} is found, *i.e.*, from 519.3 cm^{-1} to 487.5 cm^{-1}. This reduction is caused by an unconventional confinement effect, in which the phonon wave functions have nodes on the pore surfaces and consequently those with wavelengths longer than the distance between pores will not be accessible for the system, despite that the wave function are totally extended.

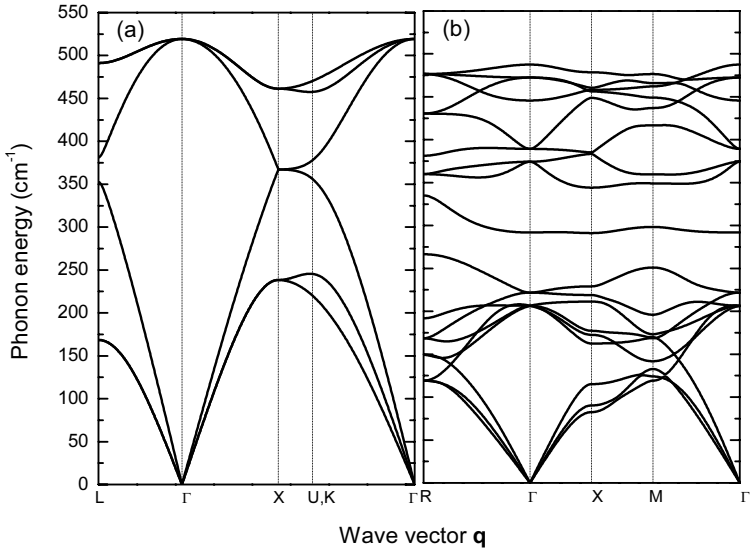

Fig. 1 Phonon dispersion relations of (a) *c*-Si and (b) PSi obtained from a 8-atom supercell with a 2-neighboring atom pore.

Figure 2(a) shows the calculated Raman peak of crystalline silicon at 519.3 cm^{-1}, very close to the experimental data [1], and the maximum Raman shifts of PSi with square pores, as shown in the insets, are presented in figures 2(b) and 2(c) for supercells of 8 and 72 atoms, respectively. Notice that the variation of these Raman peaks to lower energies is observed in PSi samples [1], in spite of the peak broadening is not reproduced, probably due to the absence of a pore-morphology distribution.

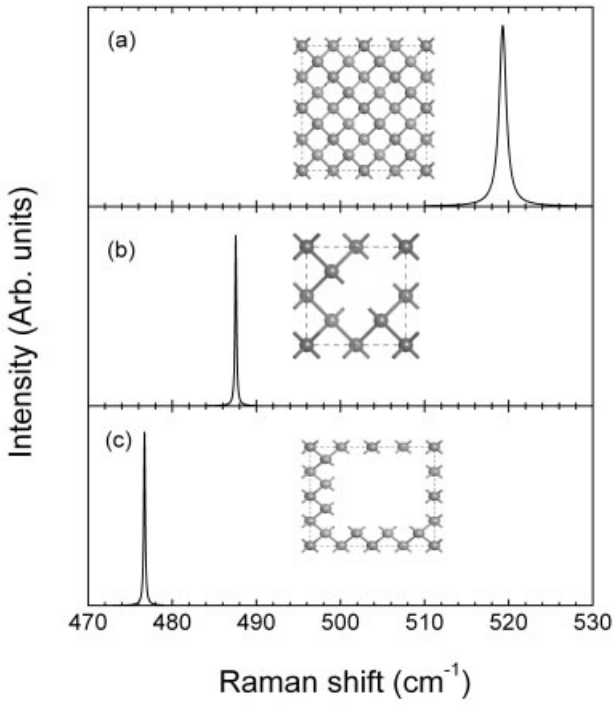

Fig. 2 Main Raman peaks for (a) c-Si, (b) and (c) PSi with 25% and 69.4% porosity, respectively.

In Fig. 3(a), the main Raman peak as a function of the porosity is shown for pores with square form, where the porosity is defined as the ratio of the number of removed Si atoms over the total number of Si atoms in the supercell. Observe that as the porosity grows these main Raman peaks asymptotically approach to 475 cm^{-1}. This fact could be understood from the significant reduction of the Brillouin zone (BZ) for large supercells and then, the BZ folding processes caused by doubling supercells have essentially no effects on the Raman response.

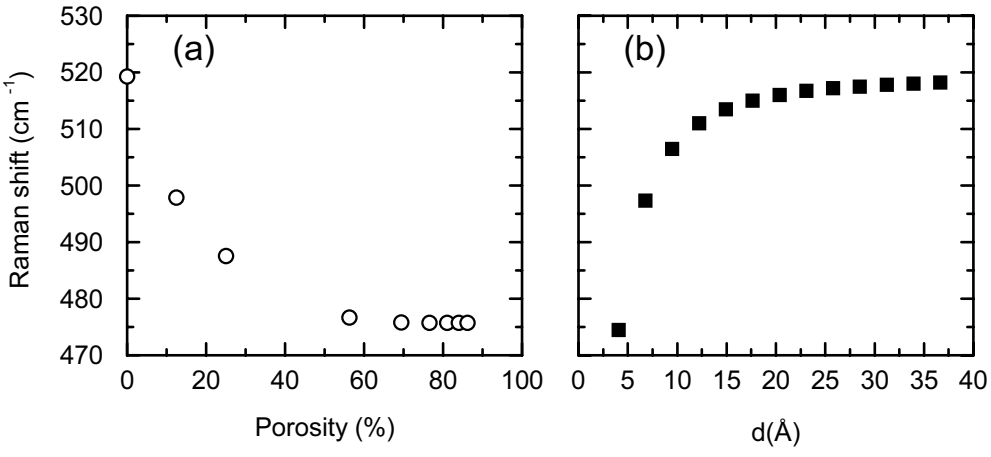

Fig. 3 Variation of the main Raman peaks (a) as a function of porosity for the square pores case, and (b) versus the cross-section width *d* for Si wires.

On the other hand, the Raman scattering in quantum wires with *c*-Si structure is also investigated, where wires with a square shape and different sizes are considered. In figure 3(b), the variation of the main Raman peak is plotted versus the width of the square wires (d). Notice that the Raman shift of quantum wires tends asymptotically to the *c*-Si value (~520 cm^{-1}), when the transversal cross section of wires grows. Moreover, for wires with smaller width the Raman shift is about 475 cm^{-1}, very close to that obtained from high porosity calculations [see Fig. 3(a)]. In fact, the remained skeleton in the supercell model has a constant width, as shown in the insets of Figs. 2(b) and 2(c). Hence, the enlargement of Raman shifts when the porosity grows is mainly due to the presence of pores, which reduces significantly the effective long-range interactions and it is decisive in the Raman scattering.

3 Conclusions

In summary, we have presented a microscopic theory to model the Raman scattering in PSi. This theory has the advantage of providing a direct relationship between the microscopic structures and the displacement-displacement coherence effects. Supercells with empty columns of Si atoms have been used to model the PSi and the Raman spectra calculated within this model are consistent with experimental data, *i.e.*, the main Raman peak shifts to lower frequencies as the porosity increases. In addition, quantum wire model is also analyzed and its results show an asymptotical behavior to the crystalline limit when the width of the wires enlarges. Contrary to the quantum wire approximation, the supercell model emphasizes the interconnection of the system, which could be relevant for long-range correlated phenomena, such as the Raman scattering.

Acknowledgements This work has been partially supported by projects CONACyT-41492F, UNAM-IN101701 UNAM-IN122704 and CGPI-IPN-20031183.

References

[1] H. Tanino, A. Kuprin, H. Deai, and N. Koshida, Phys. Rev. B **53**, 1937 (1996).
[2] R. Alben, D. Weaire, J.E. Smith, and M.H. Brodsky, Phys. Rev. B **11**, 2271 (1975).
[3] J.E. Elliott, J.A. Krumhansl, and P.L. Leath, Rev. Mod. Phys. **46**, 465 (1974).
[4] C. Wang and R.A. Barrio, Phys. Rev. Lett. **61**, 191 (1988).
[5] A.S. Carriço, R.J. Elliott, and R.A. Barrio, J. Phys. C **19**, 1113 (1986).
[6] H. Münder, C. Andrzejak, M.G. Berger, U. Klemradt, H. Lüth, R. Herino, and M. Ligeon, Thin Solid Films **221**, 27 (1992).
[7] M. Cruz, C. Wang, M.R. Beltrán, and J. Tagüeña-Martínez, Phys. Rev. B **53**, 3827 (1996).